PNAS

Supplementary Information for

Distinct neural networks derived from galanin-containing nociceptors and neurotensin-expressing pruriceptors

Yan Chen[1,3†], Yuran Song[2,3†], Huadong Wang[4†], Yiyun Zhang[5], Xinyu Hu[3,6], Kaikai Wang[3,5], Yingjin Lu[1], Zoutao Zhang[7], Shuai Li[1,3], Anan Li[7], Lan Bao[1,5,6], Fuqiang Xu[4], Changlin Li[1,3]*, and Xu Zhang[1,3,5]*

[1] Guangdong Institute of Intelligence Science and Technology, Hengqin, Zhuhai, China

[2] Institute of Neuroscience and State Key Laboratory of Neuroscience, Center for Excellence in Brain Science and Intelligence Technology, University of Chinese Academy of Sciences, CAS; Shanghai Research Center for Brain Science and Brain-Inspired Intelligence, Shanghai, China

[3] Research Unit of Pain Medicine, Chinese Academy of Medical Sciences; SIMR Joint Lab of Drug Innovation, Shanghai Advanced Research Institute, Chinese Academy of Sciences (CAS), Shanghai, China

[4] Guangdong Provincial Key Laboratory of Brain Connectome and Behavior, Brain Cognition and Brain Disease Institute, Shenzhen Institute of Advanced Technology, CAS, Shenzhen, China

[5] School of Life Science and Technology, ShanghaiTec University, Shanghai, China

[6] State Key Laboratory of Cell Biology, Shanghai Institute of Biochemistry and Cell Biology, Center for Excellence in Molecular Cell Science, CAS, Shanghai, China HUST-

[7] Suzhou Institute for Brainsmatics, JITRI Institute for Brainsmatics, Suzhou, China

†These authors contributed equally

* To whom correspondence may be addressed.Email: licl@gdiist.cn or zhangx@sari.ac.cn

This PDF file includes:

Figures S1 to S7
Tables S1 to S4
Abbreviation list
Materials and Methods
SI References

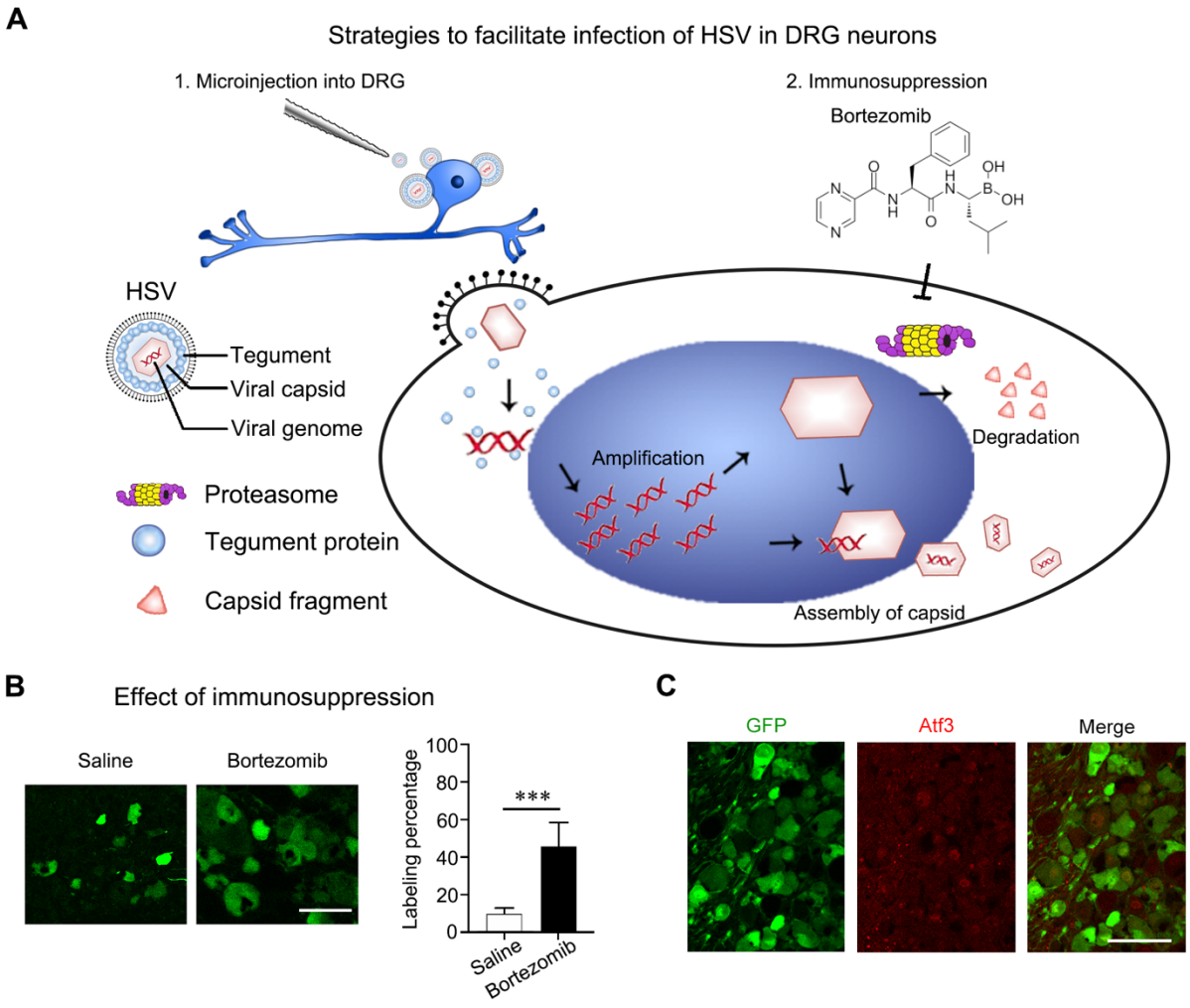
A
Strategies to facilitate infection of HSV in DRG neurons
1. Microinjection into DRG
2. Immunosuppression
Bortezomib
HSV
Tegument
Viral capsid
Viral genome
Proteasome
Tegument protein
Capsid fragment
Amplification
Degradation
Assembly of capsid
B
Effect of immunosuppression
Saline
Bortezomib
Labeling percentage
100
80
60
40
20
0
***
Saline
Bortezomib
C
GFP
Atf3
Merge

Fig. S1, Facilitation of HSV infection in DRG neurons. A, A schematic overview of two strategies to facilitate the HSV infection in DRG neurons. Left, microinjection of directly delivering the virus into DRG. The viral genome, capsid and tegument proteins could enter the soma of DRG neurons near the cell nucleus and might facilitate the initiation of viral amplification. Right, immunosuppression with bortezomib, an immunosuppressive agent to inhibit the proteasome so as to impair the degradation of viral capsids. **B,** Effect of immunosuppression in facilitating HSV infection in DRG neurons. Left, distribution of infected DRG neurons with saline or bortezomib treatment. Scale bar: 100 μm. Right, histogram showing the percentage of labeled neurons. Data was shown as mean ± SEM. (comparisons by two-tail unpaired t test: ***$P < 0.0001$, for saline 473 neurons from 23 sections/ 7 animals; for bortezomib 3811 neurons from 45 sections/ 15 animals). Bortezomib significantly increased the infection ratio of HSV. **C,** Examination of nerve injury-induced Atf3 expression after microinjection into DRG. Absence of Atf3 implied the successful microinjection without nerve injury. Scale bar: 100 μm. Microinjection didn't induce Atf3 expression in DRG.

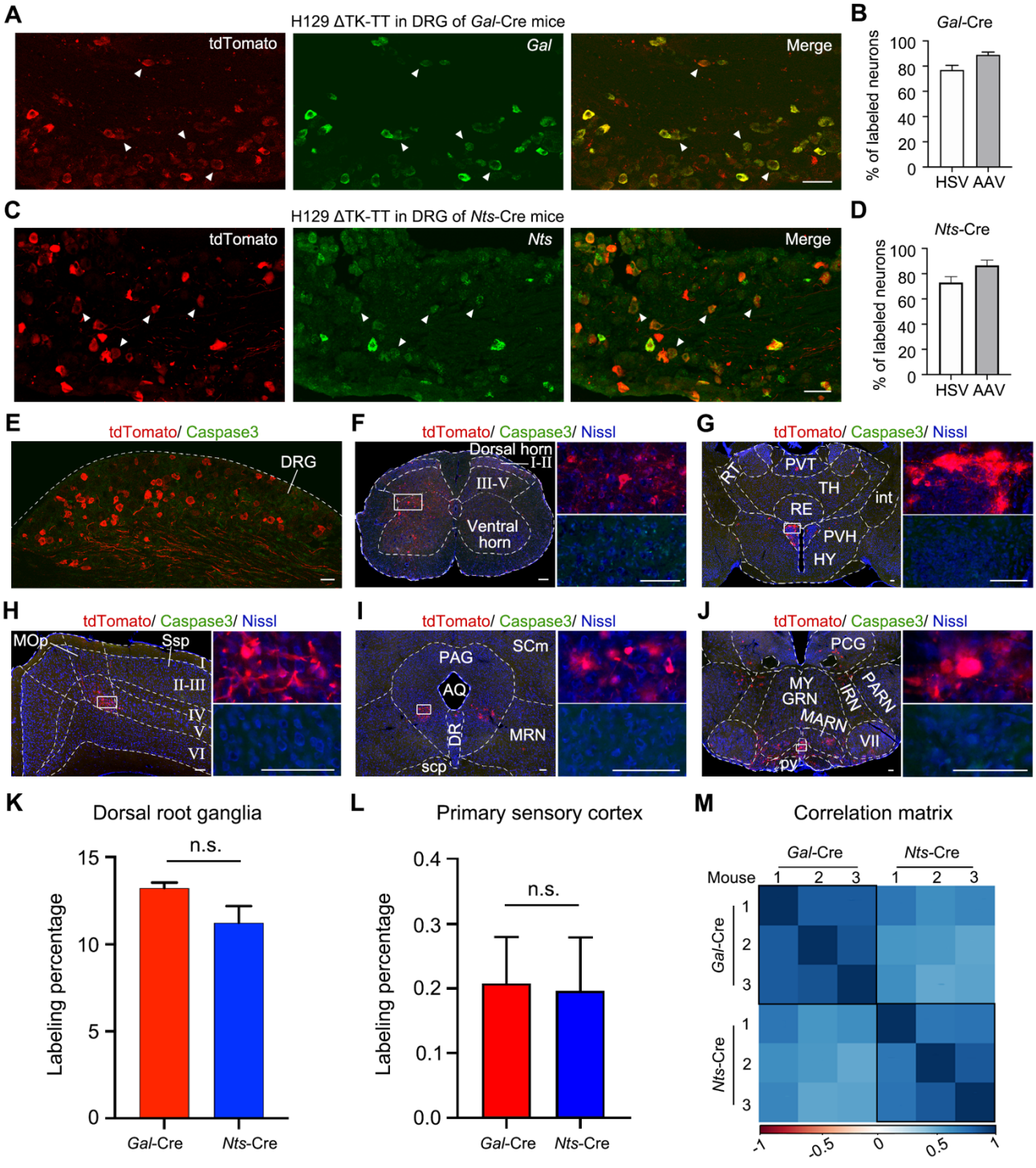

Figure S2, Chen et al., 2022

Fig. S2. Specificity of labeling, toxicity of virus and repeatability of tracing were verified. A, RNAscope ISH combined with immunohistochemistry showed co-expression of *Gal* with tdTomato in the H129ΔTK-TT infected DRG neurons of *Gal*-Cre mice. Arrows pointed out neurons expressing both *Gal* and tdTomato. Scale bar, 50 μm. **B**, Quantification of the percentage of Gal^+ neurons in virus-labeled neurons in DRG. Data was shown as mean ± SEM (for HSV labeling 230 neurons from 12 sections/ 4 animals; for AAV labeling 331 neurons from 15 sections/ 5 animals). **C**, RNAscope ISH combined with immunohistochemistry showed co-expression of *Nts* with tdTomato in the H129ΔTK-TT infected DRG neurons of *Nts*-Cre mice. Arrows pointed out neurons expressing both *Nts* and tdTomato. Scale bar, 50 μm. **D**, Quantification of the percentage of Nts^+ neurons in virus-labeled neurons in DRG. Data was shown as mean ± SEM (for HSV 308 neurons from 13 sections of 5 animals; for AAV 119 neurons from 9 sections/ 3 animals). **E-J**, Immunofluorescence showed expression of Caspase 3 (green) and viral labeling (red) in the L5 DRG, lumbar spinal cord, hypothalamus, primary motor and sensory cortex, PAG in the midbrain and medulla. No expression of caspase 3 indicated that the labeled neural networks didn't contaminate by released virus from dying neurons. **K** Quantification of the percentage of labeled neurons in injected DRG of *Gal*-Cre or *Nts*-Cre transgenic mice. Data was shown as mean ± SEM. (comparisons by two-tail unpaired t test: n.s. $P>0.05$, for *Gal*-Cre 302 neurons from 10 sections/ 3 animals, for *Nts*-Cre 268 neurons from 10 sections/ 3 animals) **L,** Quantification of the percentage of labeled neurons in SSp derived from the Gal^+ and Nts^+ DRG neurons. Data was shown as mean ± SEM. (comparisons by two-tail unpaired t test: n.s. $P>0.05$, N = 3 for each group). K and L showed that selected cases presented similar labeling percentages in DRG and SSp. **M,** Correlation matrix based

on the distribution pattern of labeled neurons in each mouse brain. The coefficient of correlation was higher within groups than those between groups.

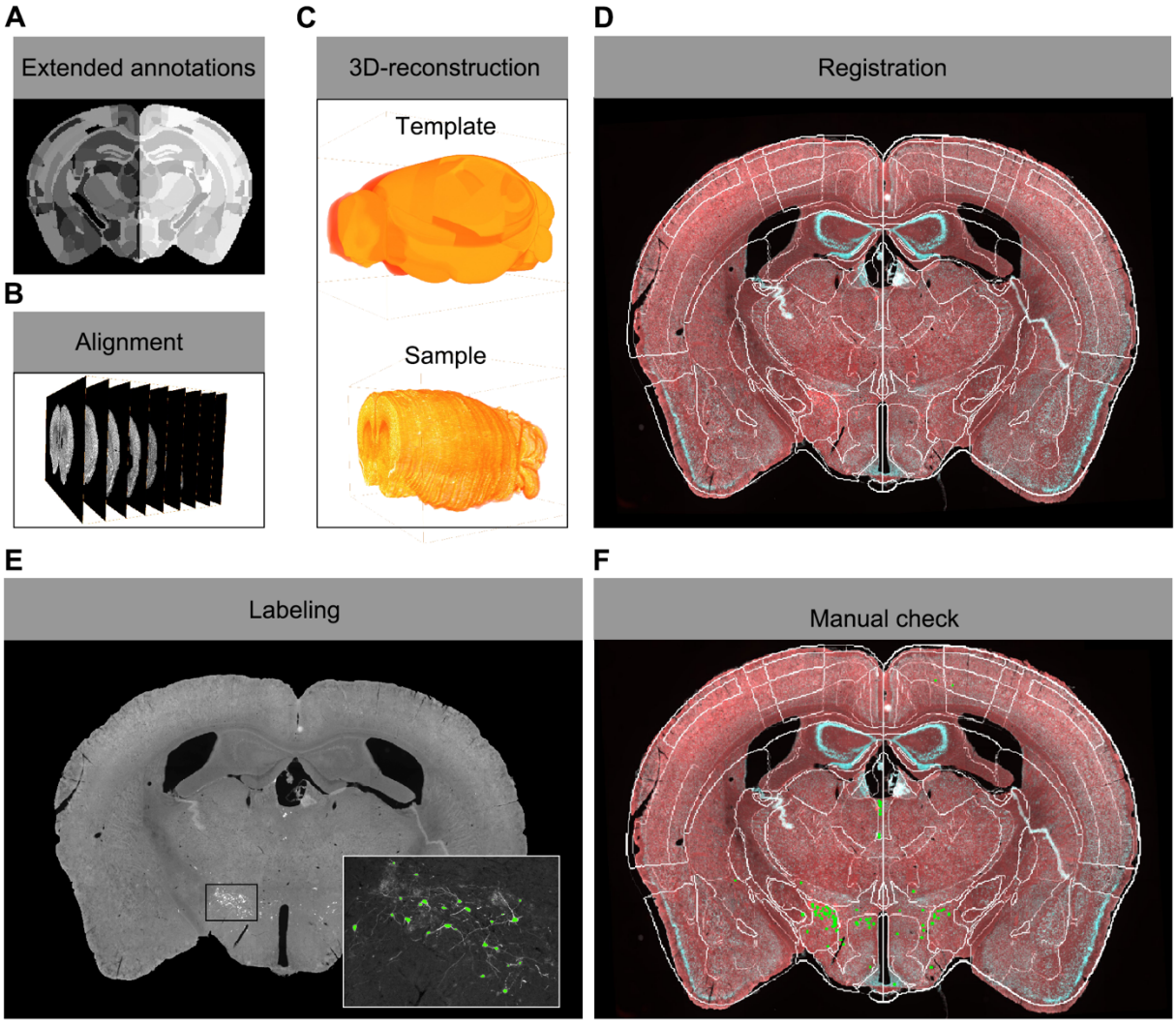
A
Extended annotations
B
Alignment
C
3D-reconstruction
Template
Sample
D
Registration
E
Labeling
F
Manual check

Fig. S3. Workflow for quantitative analysis of labeled neural networks. A, Representative slice of brain atlas with various grey values denoting each nucleus. The nuclei annotated by the 3D Allen CCFv3 were divided into two parts according to their location in the hemisphere. A total of 1014 nuclei were analyzed. **B,** The sections of a brain were aligned up for reconstruction of a three-dimension brain. **C**, Reconstruction of brain sections were registered to the Allen CCFv3. **D,** The reconstructed volume of brain sections could be well matched to the reference atlas in shape, size and position. **E,** The OTSU algorithm was applied for the image segmentation of labeled neurons in the brain. The green mask on the enlarged view represents the labeled neurons recognized by the algorithm. **F,** The interface of the software LabelMe with registered coordinate of labeled neurons presented as green dots. Fine mapping of the dots can be achieved by manually checking.

A

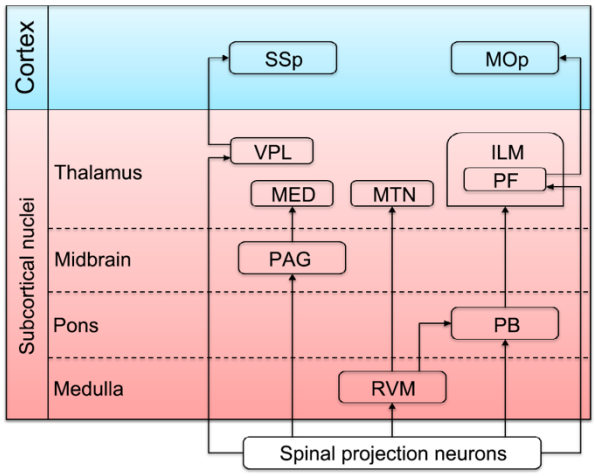

B

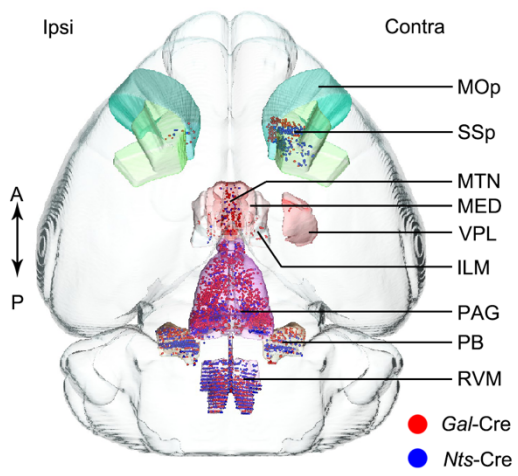

C

		Gal-Cre			*Nts*-Cre		
Total labeling number		**4395**	**6016**	**17931**	**6606**	**6954**	**19459**
CTX	SSp (Contra)	+	++	++	+	++	++
	MOp (Contra)	+++	+++	+++	++	++	++
TH	VPL (Contra)	+	+	+	-	-	-
	PF (Ipsi)	+	+	+	-	-	+
MB	PAG	+++	+++	++++	+++	+++	+++
P	PB (Ipsi)	++	++	+++	+++	+++	+++
	PB (Contra)	++	+++	+++	+++	++	+++
MY	RVM	+++	++++	++++	+++	++++	++++

+: 1-10, ++: 11-100, +++: 101-1000, ++++: > 1000

Fig. S4. Tracing of somatosensory ascending pathways. A, Schematic overview of the somatosensory ascending pathways from spinal projection neurons to subcortical nuclei and finally to the cortex. **B,** Representative top view of the three-dimension illustration showing the distribution of labeled neurons in the nuclei of somatosensory ascending pathways derived from the *Gal*$^{+}$ (red) or *Nts*$^{+}$ (blue) DRG neurons. One dot represents one labeled neuron. **C,** The number and density of labeled neurons in the nuclei of somatosensory ascending pathways. The major differences were observed in VPL and parafascicular nucleus (PF) in the thalamus.

A

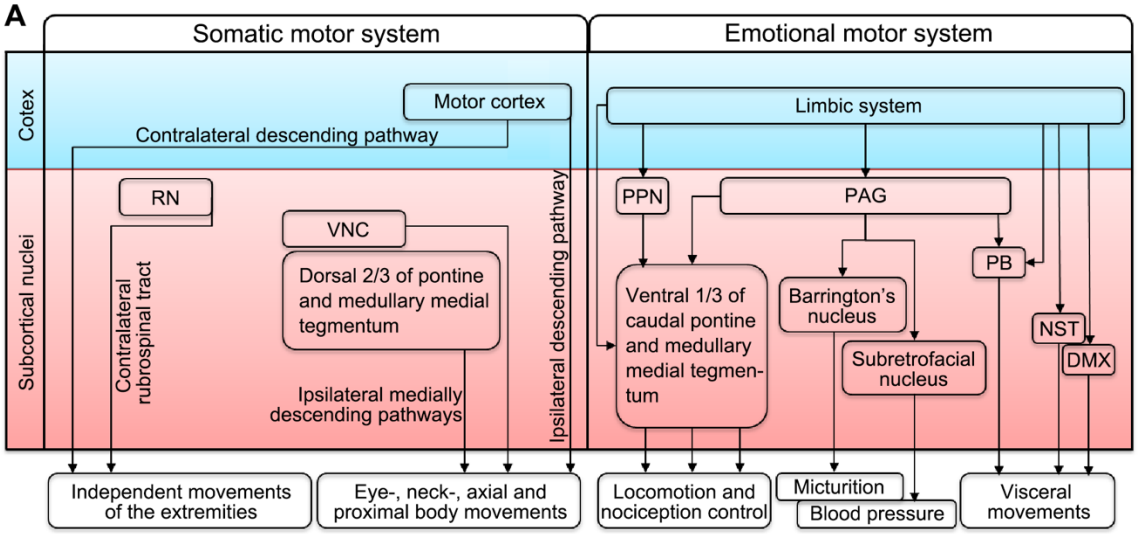

B

			Gal-Cre			*Nts*-Cre		
Total labeling number			4395	6016	17931	6606	6954	19459
Somatic motor system	Medial	VNC	++	+++	+++	++	++	+++
		PRNc	+++	+++	+++	+++	+++	+++
		GRN	+++	+++	+++	+++	+++	+++
	Lateral	RN (Contra)	+++	+++	+++	++	++	++
		RN (Ipsi)	++	++	++	+	-	+
Emotional motor system	Medial	RM	++	+++	+++	++	+++	+++
		RPA	++	++	+++	+++	+++	+++
		RO	+++	+++	+++	++	+++	+++
	Lateral	NST (Contra)	++	++	+++	+++	+++	+++
		NST (Ipsi)	++	++	+++	+++	++	+++
		DMX (Contra)	++	++	++	+++	+++	+++
		DMX (Ipsi)	++	++	+++	+++	+++	+++

+: 1-10, ++: 11-100, +++: 101-1000, ++++: > 1000

Fig. S5. Tracing of motor systems. A, Schematic overview of the motor systems including somatic motor system and emotional motor system from the cortex to control various functions. **B,** The number and density of labeled neurons in the nuclei of motor systems. The differences were observed in RN, NST and DMX.

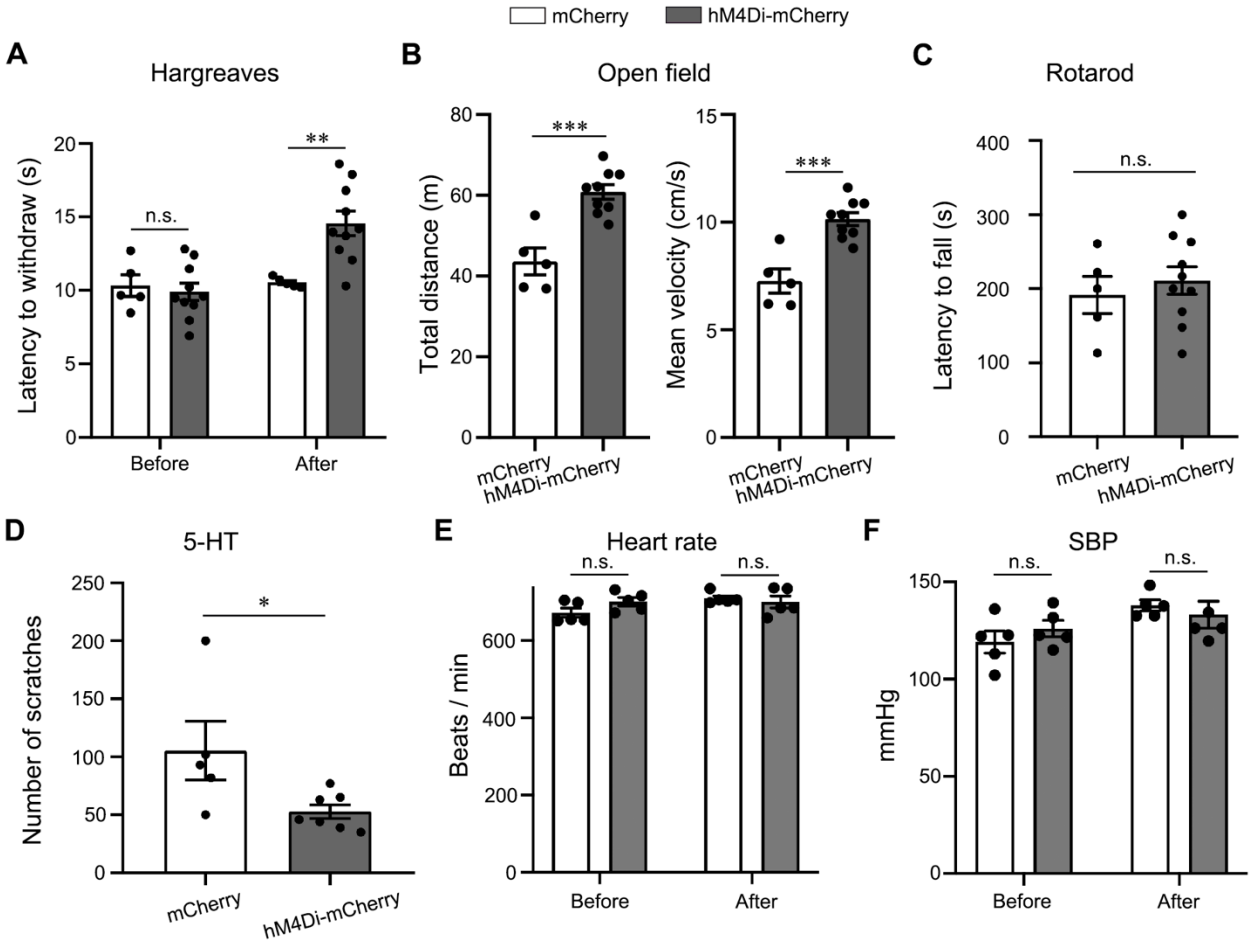
mCherry
hM4Di-mCherry
A
Hargreaves
Latency to withdraw (s)
n.s.
**
Before
After
B
Open field
Total distance (m)
***
Mean velocity (cm/s)
***
mCherry
hM4Di-mCherry
C
Rotarod
Latency to fall (s)
n.s.
mCherry
hM4Di-mCherry
D
5-HT
Number of scratches
*
mCherry
hM4Di-mCherry
E
Heart rate
Beats / min
n.s.
n.s.
Before
After
F
SBP
mmHg
n.s.
n.s.
Before
After

Fig. S6. Silencing of RN or NST/DMX impairs response to noxious heat or chemical itch, respectively. A, Hargreaves results showing significant increase of the response latency for noxious heat in mice with hM4Di expressed in the RN after CNO administration. Cut-off, 20 seconds. **B,** Results of open field test showing significant increase of the total distance of movement and mean velocity in mice with hM4Di expressed in the RN after CNO administration. **C,** Rotarod results showing that the latency to fall didn't changed when the RN was silenced. Data from **A-C** were compared by two-tail unpaired t test: ** $P < 0.005$, n.s. $P > 0.05$, N = 10 for the hM4Di group and N = 5 for control group. **A-C** indicated that silencing of the RN impairs the response of animals to noxious heat but not the motor abilities. **D**, Itch behavior test showing decreased scratching number induced by intradermal injection of 5-HT in mice with hM4Di expressed in the RN after CNO administration (comparisons by two-tail unpaired t test: * $P < 0.05$, n.s. $P > 0.05$, N = 7 for the hM4Di group and N = 5 for control group). **E** and **F**, Measurement of heart and blood pressure showing that silencing of the NST/DMX didn't affect the heart rate and systolic blood pressure of mice (comparisons by two-tail unpaired t test: * $P < 0.05$, n.s. $P > 0.05$, N = 5 for each group). **D-F** indicated that silencing of the NST/DMX impaired the response of animals to 5-HT but didn't affect the cardiovascular activity at rest state.

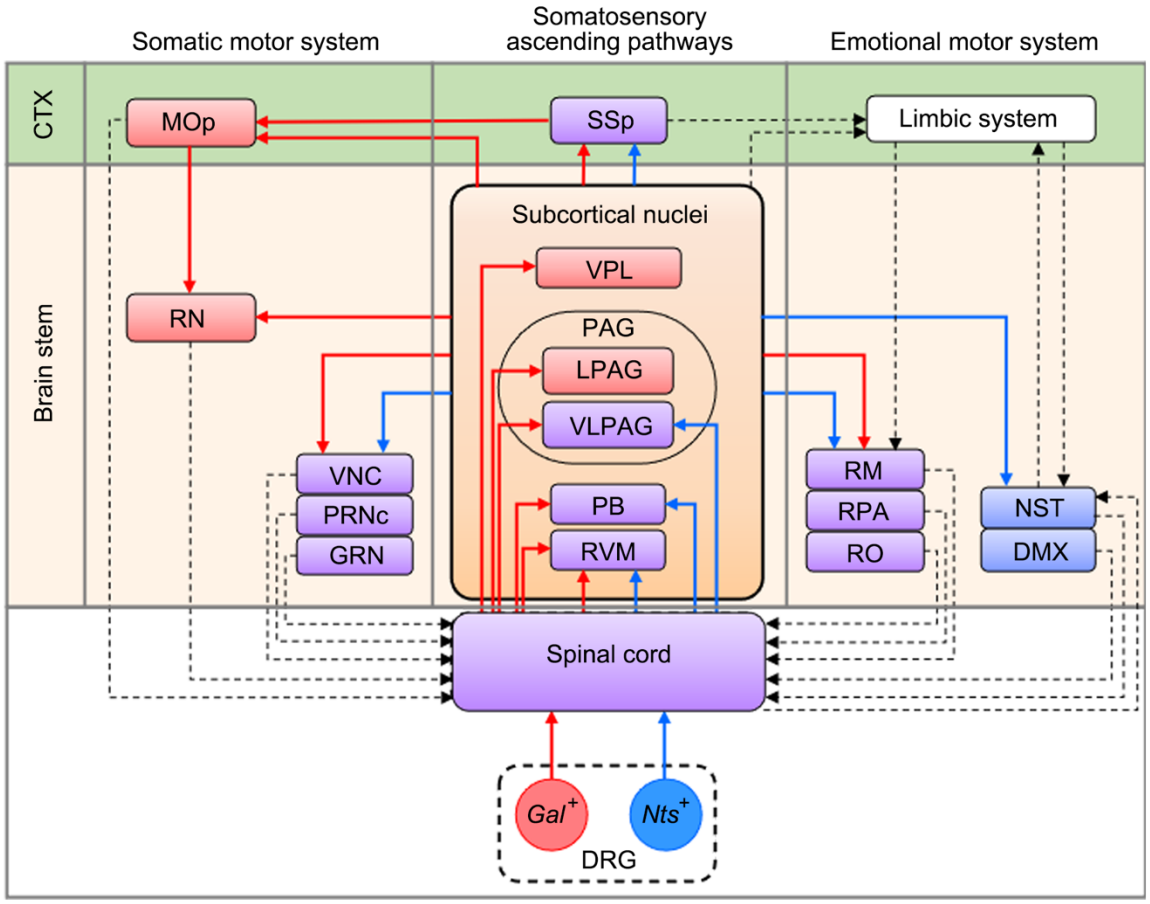
Somatic motor system
Somatosensory ascending pathways
Emotional motor system
CTX
Brain stem
MOp
SSp
Limbic system
Subcortical nuclei
VPL
RN
PAG
LPAG
VLPAG
VNC
PRNc
GRN
PB
RVM
RM
RPA
RO
NST
DMX
Spinal cord
Gal+
Nts+
DRG

Fig. S7. Schematic summary of the anatomic distinction between networks derived from *Gal*$^+$ and *Nts*$^+$ DRG neurons. Boxes in red, differentially labeled nuclei derived from the *Gal*$^+$ DRG neurons; Boxes in blue, differentially labeled nuclei derived from the *Nts*$^+$ DRG neurons; Boxes in purple, common nuclei. For ascending processing, the neural networks derived from *Gal*$^+$ nociceptors and *Nts*$^+$ pruriceptors share the spinobulbar projection but not the STT. In the motor system, the *Gal*$^+$ nociceptor-derived network tends to be more involved in the somatic motor system, while the *Nts*$^+$ pruriceptor-derived network tends to more participate in the emotional reaction. The full lines were drawn based on the data in this study, the dotted lines and the direction of arrows were drawn based on previous reports.

Table S1: Labeling percentages of constantly labeled nuclei tracing from Gal$^+$ DRG neurons

Nuclei \ Mice with Total number of labeling		*Gal*-Cre 1#	*Gal*-Cre 2#	*Gal*-Cre 3#	*Nts*-Cre 1#	*Nts*-Cre 2#	*Nts*-Cre 3#	Side
		4396	6022	17948	6607	6962	19459	
CTX	MOp5	0.159	0.050	0.061	0.000	0.000	0.021	Ipsi
	SSp-ll5	0.046	0.066	0.017	0.000	0.000	0.000	Ipsi
TH	VM	0.068	0.017	0.212	0.000	0.000	0.005	Ipsi
	VPM	0.046	0.033	0.006	0.000	0.000	0.000	Ipsi
	SPFm	0.091	0.050	0.112	0.000	0.058	0.026	Ipsi
	SPA	0.114	0.017	0.028	0.000	0.129	0.010	Ipsi
	MD	0.182	0.033	0.078	0.000	0.115	0.021	Ipsi
	PR	0.091	0.017	0.017	0.000	0.000	0.005	Ipsi
	PVT	1.206	0.100	0.234	0.045	0.259	0.062	Ipsi
	RE	0.023	0.033	0.006	0.000	0.000	0.005	Ipsi
	PF	0.250	0.017	0.033	0.000	0.000	0.021	Ipsi
	LH	0.023	0.033	0.056	0.000	0.000	0.010	Ipsi
HY	PVH	2.002	1.612	1.612	4.693	1.021	2.050	Ipsi
	PVa	0.114	0.083	0.006	0.000	0.000	0.036	Ipsi
	PVi	0.068	0.316	0.011	0.106	0.115	0.077	Ipsi
	ARH	0.023	0.166	0.022	0.015	0.029	0.062	Ipsi
	DMH	0.364	0.615	0.346	0.787	0.388	1.871	Ipsi
	AHN	0.114	0.033	0.028	0.000	0.029	0.051	Ipsi
	MPN	0.137	0.033	0.050	0.015	0.058	0.046	Ipsi
	PVHd	2.002	1.247	0.586	0.545	0.863	0.252	Ipsi
	VMH	0.296	0.116	0.123	0.000	0.086	0.041	Ipsi
	PH	1.092	0.549	1.193	0.333	0.604	0.591	Ipsi
	LHA	2.253	1.646	1.372	1.605	1.021	0.843	Ipsi
	LPO	0.137	0.017	0.078	0.000	0.129	0.062	Ipsi
	PSTN	0.501	0.066	0.178	0.000	0.000	0.021	Ipsi
	ZI	0.592	0.449	0.491	0.106	0.201	0.098	Ipsi
MB	SCop	0.023	0.033	0.045	0.015	0.000	0.000	Ipsi
	MEV	0.046	0.017	0.078	0.015	0.187	0.051	Ipsi
	VTA	0.091	0.033	0.061	0.000	0.014	0.015	Ipsi
	MRN	1.615	0.981	3.463	0.272	0.331	0.324	Ipsi
	SCdg	0.114	0.017	0.139	0.000	0.029	0.000	Ipsi
	SCiw	0.046	0.050	0.184	0.000	0.000	0.005	Ipsi
	SCig	0.046	0.017	0.123	0.000	0.014	0.015	Ipsi
	PAG	6.257	3.324	7.211	1.832	2.100	3.073	Ipsi
	ND	0.023	0.033	0.039	0.000	0.043	0.010	Ipsi

	APN	0.296	0.050	0.363	0.000	0.000	0.000	Ipsi
	NPC	0.068	0.083	0.173	0.000	0.000	0.026	Ipsi
	CUN	0.046	0.066	0.201	0.106	0.014	0.046	Ipsi
	RN	0.910	0.199	0.692	0.045	0.000	0.010	Ipsi
	EW	0.205	0.366	0.117	0.015	0.029	0.031	Ipsi
	PPN	0.228	0.216	0.703	0.257	0.072	0.108	Ipsi
	CLI	0.023	0.017	0.006	0.030	0.000	0.000	Ipsi
	DR	0.068	0.116	0.067	0.045	0.000	0.005	Ipsi
P	NLL	0.068	0.100	0.022	0.000	0.043	0.031	Ipsi
	PB	0.660	1.064	1.372	2.195	1.452	1.732	Ipsi
	KF	0.091	0.083	0.073	0.015	0.043	0.164	Ipsi
	SOCl	0.182	0.166	0.095	0.817	0.086	0.339	Ipsi
	B	0.774	0.382	0.206	0.696	0.503	0.293	Ipsi
	DTN	0.023	0.017	0.006	0.015	0.043	0.000	Ipsi
	PCG	0.501	0.266	0.446	0.409	0.316	0.627	Ipsi
	PRNc	1.456	3.474	3.090	3.118	0.647	1.609	Ipsi
	SUT	0.182	0.798	0.781	0.045	0.475	0.344	Ipsi
	CS	0.046	0.050	0.039	0.000	0.000	0.010	Ipsi
	LC	0.614	1.413	1.829	0.500	0.417	0.329	Ipsi
	LDT	0.137	0.183	0.429	0.091	0.101	0.067	Ipsi
	NI	0.023	0.033	0.006	0.030	0.000	0.015	Ipsi
	PRNr	3.254	0.831	2.794	1.302	0.618	0.612	Ipsi
	SLD	0.364	1.546	0.563	1.045	0.431	0.293	Ipsi
MY	AP	0.046	0.033	0.039	0.106	0.460	0.139	Ipsi
	CU	0.068	0.066	0.073	0.000	0.043	0.051	Ipsi
	ECU	0.023	0.017	0.045	0.015	0.000	0.021	Ipsi
	NTS	0.728	0.981	0.909	3.300	2.013	0.848	Ipsi
	SPVI	0.046	0.100	0.112	0.000	0.000	0.093	Ipsi
	VII	0.182	0.682	0.190	1.847	0.604	1.151	Ipsi
	DMX	0.660	0.615	0.502	3.134	2.114	0.622	Ipsi
	GRN	3.094	3.657	2.320	1.620	2.028	3.212	Ipsi
	IO	0.819	0.017	0.346	0.378	3.207	0.452	Ipsi
	IRN	1.115	1.828	2.220	3.330	3.638	2.071	Ipsi
	LRNm	0.728	0.399	0.547	0.469	4.645	1.192	Ipsi
	MARN	1.502	3.574	2.565	1.938	2.272	3.649	Ipsi
	MDRNd	0.159	0.183	0.245	0.167	0.216	0.062	Ipsi
	MDRNv	0.819	0.449	0.273	0.923	0.446	0.349	Ipsi
	PARN	0.569	0.731	1.283	1.029	0.201	0.468	Ipsi
	PGRNl	3.914	2.942	2.275	2.816	9.189	5.822	Ipsi
	PRP	0.228	0.033	0.312	0.197	0.316	0.128	Ipsi
	PPY	0.432	0.947	0.340	1.029	0.446	1.470	Ipsi
	MV	0.865	0.947	1.154	0.530	0.475	0.925	Ipsi
	SPIV	0.091	0.116	0.502	0.015	0.000	0.067	Ipsi
	SUV	0.091	0.316	0.290	0.015	0.144	0.015	Ipsi
	x	0.046	0.100	0.011	0.000	0.000	0.005	Ipsi

	XII	0.023	0.116	0.028	0.061	0.058	0.200	Ipsi
	RM	1.160	1.679	0.323	0.348	1.237	1.038	Ipsi
	RPA	0.751	0.898	0.402	0.969	1.553	0.822	Ipsi
	RO	1.229	1.828	0.195	0.288	1.366	0.668	Ipsi
CB	CENT2	0.319	0.133	0.067	0.015	0.000	0.021	Ipsi
	CENT3	0.296	0.249	0.128	0.030	0.000	0.082	Ipsi
	CUL4-5	0.159	0.133	0.329	0.045	0.000	0.015	Ipsi
	DEC	0.068	0.050	0.162	0.000	0.000	0.000	Ipsi
	PYR	0.023	0.050	0.011	0.000	0.000	0.000	Ipsi
	SIM	0.023	0.033	0.151	0.015	0.000	0.005	Ipsi
	ANcr1	0.046	0.017	0.139	0.015	0.000	0.015	Ipsi
	ANcr2	0.046	0.017	0.056	0.000	0.000	0.000	Ipsi
	FN	0.023	0.199	0.145	0.015	0.000	0.000	Ipsi
	IP	0.023	0.166	0.218	0.076	0.014	0.010	Ipsi
CTX	MOp5	2.321	1.695	0.742	0.151	0.331	0.391	Contra
	SSp-ll5	0.159	0.332	0.117	0.045	0.216	0.324	Contra
CNU	CEAm	0.023	0.033	0.017	0.000	0.000	0.000	Contra
TH	VPL	0.341	0.050	0.017	0.000	0.000	0.000	Contra
	VPM	0.068	0.017	0.011	0.000	0.000	0.000	Contra
	SPA	0.068	0.033	0.006	0.015	0.058	0.000	Contra
	PO	0.046	0.199	0.006	0.000	0.000	0.000	Contra
	IMD	0.023	0.066	0.011	0.000	0.000	0.021	Contra
	MD	0.046	0.050	0.045	0.015	0.014	0.000	Contra
	PVT	0.819	0.449	0.195	0.015	0.201	0.041	Contra
HY	PVH	0.614	0.399	0.424	1.241	0.345	0.421	Contra
	PVi	0.091	0.017	0.011	0.045	0.014	0.031	Contra
	ARH	0.046	0.017	0.022	0.000	0.014	0.026	Contra
	DMH	0.205	0.216	0.268	0.530	0.561	0.278	Contra
	MPO	0.023	0.050	0.084	0.015	0.086	0.031	Contra
	AHN	0.114	0.050	0.039	0.000	0.000	0.000	Contra
	MPN	0.091	0.017	0.028	0.000	0.029	0.021	Contra
	PVHd	0.341	0.283	0.106	0.257	0.417	0.108	Contra
	VMH	0.137	0.083	0.039	0.000	0.014	0.015	Contra
	PH	0.910	0.482	1.093	0.288	0.345	0.678	Contra
	LHA	1.047	0.316	0.770	0.469	0.244	0.236	Contra
	LPO	0.046	0.017	0.022	0.000	0.000	0.108	Contra
	PSTN	0.182	0.066	0.028	0.030	0.000	0.000	Contra
	TU	0.046	0.017	0.011	0.030	0.043	0.010	Contra
	ZI	0.273	0.199	0.117	0.000	0.029	0.031	Contra
	FF	0.023	0.066	0.073	0.000	0.000	0.000	Contra
MB	ICc	0.023	0.100	0.006	0.000	0.000	0.015	Contra
	SNr	0.023	0.017	0.045	0.000	0.000	0.000	Contra
	VTA	0.046	0.033	0.033	0.030	0.043	0.005	Contra
	MRN	1.797	1.280	1.818	0.212	0.575	0.313	Contra
	SCdg	0.046	0.050	0.067	0.000	0.000	0.000	Contra

	SCig	0.046	0.017	0.056	0.000	0.000	0.005	Contra
	PAG	4.460	4.521	4.004	1.393	1.395	2.035	Contra
	PRC	0.182	0.050	0.078	0.000	0.000	0.000	Contra
	APN	0.455	0.066	0.245	0.015	0.000	0.000	Contra
	RN	3.003	2.527	1.099	0.303	0.302	0.411	Contra
	EW	0.182	0.499	0.184	0.030	0.000	0.026	Contra
	PPN	0.228	0.283	0.284	0.167	0.043	0.031	Contra
	IF	0.023	0.033	0.006	0.000	0.000	0.000	Contra
	DR	0.023	0.050	0.061	0.015	0.000	0.031	Contra
P	PB	0.683	1.080	0.680	1.559	0.820	0.714	Contra
	SOCl	0.159	0.050	0.089	0.363	0.058	0.005	Contra
	B	0.182	0.183	0.173	0.348	0.129	0.216	Contra
	PCG	0.296	0.532	0.156	0.227	0.345	0.334	Contra
	PRNc	2.253	2.610	1.896	2.301	0.892	0.961	Contra
	SUT	0.273	0.266	0.435	0.272	0.216	0.349	Contra
	V	0.023	0.233	0.045	0.030	0.000	0.093	Contra
	LC	0.273	0.898	0.876	0.424	0.374	0.298	Contra
	LDT	0.023	0.166	0.212	0.151	0.345	0.031	Contra
	PRNr	2.435	1.280	2.130	1.347	0.618	0.498	Contra
	RPO	0.046	0.033	0.017	0.030	0.000	0.000	Contra
	SLD	0.296	1.180	0.441	0.787	0.403	0.319	Contra
MY	AP	0.023	0.050	0.022	0.030	0.216	0.021	Contra
	NTS	0.296	0.848	0.641	2.165	1.251	0.653	Contra
	SPVI	0.023	0.066	0.134	0.015	0.029	0.026	Contra
	VII	0.205	0.449	0.095	1.877	0.273	0.498	Contra
	DMX	0.205	0.914	0.463	3.239	1.438	0.555	Contra
	GRN	2.503	2.061	1.545	1.287	1.194	1.567	Contra
	IO	0.933	0.033	0.212	0.363	2.502	0.370	Contra
	IRN	0.887	1.213	1.863	3.270	2.617	2.179	Contra
	LRNm	0.910	0.116	0.424	0.590	2.387	0.719	Contra
	MARN	1.320	2.443	1.528	2.089	1.524	2.590	Contra
	MDRNd	0.182	0.183	0.190	0.106	0.158	0.026	Contra
	MDRNv	0.387	0.199	0.374	0.378	0.647	0.288	Contra
	PARN	0.319	0.565	0.814	0.500	0.115	0.452	Contra
	PGRNl	2.548	1.878	1.662	2.679	4.832	4.044	Contra
	PRP	0.023	0.050	0.223	0.182	0.259	0.344	Contra
	PPY	0.091	0.332	0.323	0.590	0.259	0.699	Contra
	MV	0.364	0.582	0.719	0.363	0.129	0.632	Contra
	SPIV	0.023	0.233	0.379	0.015	0.000	0.057	Contra
	SUV	0.068	0.050	0.078	0.030	0.000	0.000	Contra
	XII	0.023	0.116	0.039	0.015	0.029	0.118	Contra
	RM	0.705	1.097	0.508	0.802	0.661	0.863	Contra
	RPA	0.796	0.549	0.402	1.544	0.906	0.637	Contra
	RO	1.274	0.515	0.407	1.196	0.230	0.719	Contra
CB	CENT2	0.182	0.150	0.084	0.000	0.000	0.057	Contra

	CENT3	0.205	0.050	0.117	0.045	0.000	0.026	Contra
	CUL4-5	0.046	0.116	0.251	0.000	0.000	0.021	Contra
	PYR	0.023	0.017	0.017	0.000	0.000	0.000	Contra
	ANcr1	0.068	0.050	0.039	0.000	0.000	0.000	Contra
	IP	0.023	0.050	0.156	0.015	0.000	0.015	Contra

The abbreviation of nuclei refers to the annotation of the Allen Adult Mouse Atlases (http://atlas.brain-map.org/).

Table S2: Labeling percentages of constantly labeled nuclei tracing from Nts$^+$ DRG neurons

Mice with Total number of labeling / Nuclei		*Gal*-Cre 1#	*Gal*-Cre 2#	*Gal*-Cre 3#	*Nts*-Cre 1#	*Nts*-Cre 2#	*Nts*-Cre 3#	Side
		4396	6022	17948	6607	6962	19459	
CNU	BST	0.205	0.000	0.078	0.045	0.086	0.031	Ipsi
TH	PVT	1.206	0.100	0.234	0.045	0.259	0.062	Ipsi
HY	PVH	2.002	1.612	1.612	4.693	1.021	2.050	Ipsi
	PVi	0.068	0.316	0.011	0.106	0.115	0.077	Ipsi
	ARH	0.023	0.166	0.022	0.015	0.029	0.062	Ipsi
	DMH	0.364	0.615	0.346	0.787	0.388	1.871	Ipsi
	MPO	0.205	0.000	0.128	0.045	0.129	0.010	Ipsi
	MPN	0.137	0.033	0.050	0.015	0.058	0.046	Ipsi
	PVHd	2.002	1.247	0.586	0.545	0.863	0.252	Ipsi
	PH	1.092	0.549	1.193	0.333	0.604	0.591	Ipsi
	LHA	2.253	1.646	1.372	1.605	1.021	0.843	Ipsi
	RCH	0.000	0.000	0.011	0.030	0.086	0.026	Ipsi
	ZI	0.592	0.449	0.491	0.106	0.201	0.098	Ipsi
MB	ICd	0.068	0.000	0.156	0.061	0.029	0.036	Ipsi
	MEV	0.046	0.017	0.078	0.015	0.187	0.051	Ipsi
	RR	0.000	0.083	0.128	0.045	0.072	0.278	Ipsi
	MRN	1.615	0.981	3.463	0.272	0.331	0.324	Ipsi
	PAG	6.257	3.324	7.211	1.832	2.100	3.073	Ipsi
	PRC	0.023	0.000	0.095	0.015	0.029	0.010	Ipsi
	CUN	0.046	0.066	0.201	0.106	0.014	0.046	Ipsi
	EW	0.205	0.366	0.117	0.015	0.029	0.031	Ipsi
	PPN	0.228	0.216	0.703	0.257	0.072	0.108	Ipsi
P	PSV	0.000	0.000	0.028	0.015	0.014	0.021	Ipsi
	PB	0.660	1.064	1.372	2.195	1.452	1.732	Ipsi
	KF	0.091	0.083	0.073	0.015	0.043	0.164	Ipsi
	SOCm	0.000	0.000	0.000	0.045	0.029	0.021	Ipsi
	SOCl	0.182	0.166	0.095	0.817	0.086	0.339	Ipsi
	B	0.774	0.382	0.206	0.696	0.503	0.293	Ipsi
	PCG	0.501	0.266	0.446	0.409	0.316	0.627	Ipsi
	PRNc	1.456	3.474	3.090	3.118	0.647	1.609	Ipsi
	SUT	0.182	0.798	0.781	0.045	0.475	0.344	Ipsi
	V	0.000	0.066	0.100	0.030	0.014	0.093	Ipsi
	LC	0.614	1.413	1.829	0.500	0.417	0.329	Ipsi
	LDT	0.137	0.183	0.429	0.091	0.101	0.067	Ipsi
	PRNr	3.254	0.831	2.794	1.302	0.618	0.612	Ipsi
	SLC	0.000	1.463	1.071	1.075	0.633	0.134	Ipsi

	SLD	0.364	1.546	0.563	1.045	0.431	0.293	Ipsi
MY	AP	0.046	0.033	0.039	0.106	0.460	0.139	Ipsi
	NTS	0.728	0.981	0.909	3.300	2.013	0.848	Ipsi
	VII	0.182	0.682	0.190	1.847	0.604	1.151	Ipsi
	AMBv	0.000	0.133	0.000	0.061	0.129	0.077	Ipsi
	DMX	0.660	0.615	0.502	3.134	2.114	0.622	Ipsi
	GRN	3.094	3.657	2.320	1.620	2.028	3.212	Ipsi
	IO	0.819	0.017	0.346	0.378	3.207	0.452	Ipsi
	IRN	1.115	1.828	2.220	3.330	3.638	2.071	Ipsi
	LRNm	0.728	0.399	0.547	0.469	4.645	1.192	Ipsi
	MARN	1.502	3.574	2.565	1.938	2.272	3.649	Ipsi
	MDRNd	0.159	0.183	0.245	0.167	0.216	0.062	Ipsi
	MDRNv	0.819	0.449	0.273	0.923	0.446	0.349	Ipsi
	PARN	0.569	0.731	1.283	1.029	0.201	0.468	Ipsi
	PGRNd	0.000	0.000	0.178	0.409	0.115	0.247	Ipsi
	PGRNl	3.914	2.942	2.275	2.816	9.189	5.822	Ipsi
	PRP	0.228	0.033	0.312	0.197	0.316	0.128	Ipsi
	PPY	0.432	0.947	0.340	1.029	0.446	1.470	Ipsi
	MV	0.865	0.947	1.154	0.530	0.475	0.925	Ipsi
	SUV	0.091	0.316	0.290	0.015	0.144	0.015	Ipsi
	XII	0.023	0.116	0.028	0.061	0.058	0.200	Ipsi
	RM	1.160	1.679	0.323	0.348	1.237	1.038	Ipsi
	RPA	0.751	0.898	0.402	0.969	1.553	0.822	Ipsi
	RO	1.229	1.828	0.195	0.288	1.366	0.668	Ipsi
CB	IP	0.023	0.166	0.218	0.076	0.014	0.010	Ipsi
CTX	MOp5	2.321	1.695	0.742	0.151	0.331	0.391	Contra
	SSp-ll5	0.159	0.332	0.117	0.045	0.216	0.324	Contra
	SSp-tr5	0.000	0.017	0.017	0.015	0.029	0.154	Contra
TH	PVT	0.819	0.449	0.195	0.015	0.201	0.041	Contra
HY	PVH	0.614	0.399	0.424	1.241	0.345	0.421	Contra
	PVi	0.091	0.017	0.011	0.045	0.014	0.031	Contra
	AVPV	0.023	0.000	0.000	0.045	0.029	0.005	Contra
	DMH	0.205	0.216	0.268	0.530	0.561	0.278	Contra
	MPO	0.023	0.050	0.084	0.015	0.086	0.031	Contra
	PVHd	0.341	0.283	0.106	0.257	0.417	0.108	Contra
	PH	0.910	0.482	1.093	0.288	0.345	0.678	Contra
	LHA	1.047	0.316	0.770	0.469	0.244	0.236	Contra
	TU	0.046	0.017	0.011	0.030	0.043	0.010	Contra
MB	VTA	0.046	0.033	0.033	0.030	0.043	0.005	Contra
	MRN	1.797	1.280	1.818	0.212	0.575	0.313	Contra
	PAG	4.460	4.521	4.004	1.393	1.395	2.035	Contra
	NPC	0.137	0.000	0.073	0.045	0.014	0.005	Contra
	CUN	0.000	0.083	0.061	0.091	0.014	0.021	Contra
	RN	3.003	2.527	1.099	0.303	0.302	0.411	Contra
	PPN	0.228	0.283	0.284	0.167	0.043	0.031	Contra

P	PSV	0.000	0.033	0.022	0.015	0.029	0.015	Contra
	PB	0.683	1.080	0.680	1.559	0.820	0.714	Contra
	SOCl	0.159	0.050	0.089	0.363	0.058	0.005	Contra
	B	0.182	0.183	0.173	0.348	0.129	0.216	Contra
	PCG	0.296	0.532	0.156	0.227	0.345	0.334	Contra
	PG	0.023	0.000	0.084	0.061	0.029	0.010	Contra
	PRNc	2.253	2.610	1.896	2.301	0.892	0.961	Contra
	SUT	0.273	0.266	0.435	0.272	0.216	0.349	Contra
	LC	0.273	0.898	0.876	0.424	0.374	0.298	Contra
	LDT	0.023	0.166	0.212	0.151	0.345	0.031	Contra
	NI	0.046	0.000	0.033	0.030	0.014	0.010	Contra
	PRNr	2.435	1.280	2.130	1.347	0.618	0.498	Contra
	SLC	0.000	1.280	0.719	0.711	0.288	0.894	Contra
	SLD	0.296	1.180	0.441	0.787	0.403	0.319	Contra
MY	AP	0.023	0.050	0.022	0.030	0.216	0.021	Contra
	NTS	0.296	0.848	0.641	2.165	1.251	0.653	Contra
	SPVI	0.023	0.066	0.134	0.015	0.029	0.026	Contra
	VII	0.205	0.449	0.095	1.877	0.273	0.498	Contra
	DMX	0.205	0.914	0.463	3.239	1.438	0.555	Contra
	GRN	2.503	2.061	1.545	1.287	1.194	1.567	Contra
	IO	0.933	0.033	0.212	0.363	2.502	0.370	Contra
	IRN	0.887	1.213	1.863	3.270	2.617	2.179	Contra
	LRNm	0.910	0.116	0.424	0.590	2.387	0.719	Contra
	MARN	1.320	2.443	1.528	2.089	1.524	2.590	Contra
	MDRNd	0.182	0.183	0.190	0.106	0.158	0.026	Contra
	MDRNv	0.387	0.199	0.374	0.378	0.647	0.288	Contra
	PARN	0.319	0.565	0.814	0.500	0.115	0.452	Contra
	PGRNd	0.023	0.000	0.502	0.182	0.058	0.355	Contra
	PGRNl	2.548	1.878	1.662	2.679	4.832	4.044	Contra
	PRP	0.023	0.050	0.223	0.182	0.259	0.344	Contra
	PPY	0.091	0.332	0.323	0.590	0.259	0.699	Contra
	MV	0.364	0.582	0.719	0.363	0.129	0.632	Contra
	XII	0.023	0.116	0.039	0.015	0.029	0.118	Contra
	RM	0.705	1.097	0.508	0.802	0.661	0.863	Contra
	RPA	0.796	0.549	0.402	1.544	0.906	0.637	Contra
	RO	1.274	0.515	0.407	1.196	0.230	0.719	Contra
CB	FN	0.000	0.066	0.095	0.030	0.014	0.015	Contra

The abbreviation of nuclei refers to the annotation of the Allen Adult Mouse Atlases (http://atlas.brain-map.org/).

Table S3: Labeling percentages of differentially labeled nuclei

Nuclei \ Mice with Total number of labeling		*Gal*-Cre 1#	*Gal*-Cre 2#	*Gal*-Cre 3#	*Nts*-Cre 1#	*Nts*-Cre 2#	*Nts*-Cre 3#	Type of network
		4396	6022	17948	6607	6962	19459	
CTX	MOp5_ipsi	0.159	0.050	0.061	0.000	0.000	0.021	Gal
	SSp-ll5_ipsi	0.046	0.066	0.017	0.000	0.000	0.000	Gal
	SSp-tr5_contra	0.068	0.017	0.212	0.000	0.000	0.005	Nts
CNU	CEAm_contra	0.046	0.033	0.006	0.000	0.000	0.000	Gal
TH	VM_ipsi	0.091	0.050	0.112	0.000	0.058	0.026	Gal
	VPM_ipsi	0.114	0.017	0.028	0.000	0.129	0.010	Gal
	SPFm_ipsi	0.182	0.033	0.078	0.000	0.115	0.021	Gal
	MD_ipsi	0.091	0.017	0.017	0.000	0.000	0.005	Gal
	PR_ipsi	1.206	0.100	0.234	0.045	0.259	0.062	Gal
	RE_ipsi	0.023	0.033	0.006	0.000	0.000	0.005	Gal
	PF_ipsi	0.250	0.017	0.033	0.000	0.000	0.021	Gal
	LH_ipsi	0.023	0.033	0.056	0.000	0.000	0.010	Gal
	VPL_contra	2.002	1.612	1.612	4.693	1.021	2.050	Gal
	VPM_contra	0.114	0.083	0.006	0.000	0.000	0.036	Gal
	PO_contra	0.068	0.316	0.011	0.106	0.115	0.077	Gal
	IMD_contra	0.023	0.166	0.022	0.015	0.029	0.062	Gal
	MD_contra	0.364	0.615	0.346	0.787	0.388	1.871	Gal
HY	PVa_ipsi	0.114	0.033	0.028	0.000	0.029	0.051	Gal
	AHN_ipsi	0.137	0.033	0.050	0.015	0.058	0.046	Gal
	VMH_ipsi	2.002	1.247	0.586	0.545	0.863	0.252	Gal
	PSTN_ipsi	0.296	0.116	0.123	0.000	0.086	0.041	Gal
	ARH_contra	1.092	0.549	1.193	0.333	0.604	0.591	Gal
	AHN_contra	2.253	1.646	1.372	1.605	1.021	0.843	Gal
	MPN_contra	0.137	0.017	0.078	0.000	0.129	0.062	Gal
	VMH_contra	0.501	0.066	0.178	0.000	0.000	0.021	Gal
	PSTN_contra	0.592	0.449	0.491	0.106	0.201	0.098	Gal
	ZI_contra	0.023	0.033	0.045	0.015	0.000	0.000	Gal
	FF_contra	0.046	0.017	0.078	0.015	0.187	0.051	Gal
	ZI_ipsi	0.091	0.033	0.061	0.000	0.014	0.015	Gal
	RCH_ipsi	1.615	0.981	3.463	0.272	0.331	0.324	Nts
	AVPV_contra	0.114	0.017	0.139	0.000	0.029	0.000	Nts
MB	SCop_ipsi	0.046	0.050	0.184	0.000	0.000	0.005	Gal
	VTA_ipsi	0.046	0.017	0.123	0.000	0.014	0.015	Gal
	SCdg_ipsi	6.257	3.324	7.211	1.832	2.100	3.073	Gal
	SCiw_ipsi	0.023	0.033	0.039	0.000	0.043	0.010	Gal
	SCig_ipsi	0.296	0.050	0.363	0.000	0.000	0.000	Gal
	APN_ipsi	0.068	0.083	0.173	0.000	0.000	0.026	Gal
	NPC_ipsi	0.046	0.066	0.201	0.106	0.014	0.046	Gal
	RN_ipsi	0.910	0.199	0.692	0.045	0.000	0.010	Gal
	DR_ipsi	0.205	0.366	0.117	0.015	0.029	0.031	Gal
	ICc_contra	0.228	0.216	0.703	0.257	0.072	0.108	Gal

	SNr_contra	0.023	0.017	0.006	0.030	0.000	0.000	Gal
	SCdg_contra	0.068	0.116	0.067	0.045	0.000	0.005	Gal
	SCig_contra	0.068	0.100	0.022	0.000	0.043	0.031	Gal
	PRC_contra	0.660	1.064	1.372	2.195	1.452	1.732	Gal
	APN_contra	0.091	0.083	0.073	0.015	0.043	0.164	Gal
	EW_contra	0.182	0.166	0.095	0.817	0.086	0.339	Gal
	IF_contra	0.774	0.382	0.206	0.696	0.503	0.293	Gal
	DR_contra	0.023	0.017	0.006	0.015	0.043	0.000	Gal
	MRN_contra	0.501	0.266	0.446	0.409	0.316	0.627	Gal
	PAG_contra	1.456	3.474	3.090	3.118	0.647	1.609	Gal
	PPN_contra	0.182	0.798	0.781	0.045	0.475	0.344	Gal
P	NLL_ipsi	0.046	0.050	0.039	0.000	0.000	0.010	Gal
	CS_ipsi	0.614	1.413	1.829	0.500	0.417	0.329	Gal
	V_contra	0.137	0.183	0.429	0.091	0.101	0.067	Gal
	RPO_contra	0.023	0.033	0.006	0.030	0.000	0.015	Gal
	SOCm_ipsi	3.254	0.831	2.794	1.302	0.618	0.612	Nts
MY	CU_ipsi	0.364	1.546	0.563	1.045	0.431	0.293	Gal
	ECU_ipsi	0.046	0.033	0.039	0.106	0.460	0.139	Gal
	SPVI_ipsi	0.068	0.066	0.073	0.000	0.043	0.051	Gal
	SPIV_ipsi	0.023	0.017	0.045	0.015	0.000	0.021	Gal
	x_ipsi	0.728	0.981	0.909	3.300	2.013	0.848	Gal
	SPIV_contra	0.046	0.100	0.112	0.000	0.000	0.093	Gal
	SUV_contra	0.182	0.682	0.190	1.847	0.604	1.151	Gal
	IRN_contra	0.660	0.615	0.502	3.134	2.114	0.622	Nts
	AMBv_ipsi	3.094	3.657	2.320	1.620	2.028	3.212	Nts
	PGRNd_ipsi	0.819	0.017	0.346	0.378	3.207	0.452	Nts
CB	CENT2_ipsi	1.115	1.828	2.220	3.330	3.638	2.071	Gal
	CENT3_ipsi	0.728	0.399	0.547	0.469	4.645	1.192	Gal
	CUL4-5_ipsi	1.502	3.574	2.565	1.938	2.272	3.649	Gal
	DEC_ipsi	0.159	0.183	0.245	0.167	0.216	0.062	Gal
	PYR_ipsi	0.819	0.449	0.273	0.923	0.446	0.349	Gal
	SIM_ipsi	0.569	0.731	1.283	1.029	0.201	0.468	Gal
	ANcr1_ipsi	3.914	2.942	2.275	2.816	9.189	5.822	Gal
	ANcr2_ipsi	0.228	0.033	0.312	0.197	0.316	0.128	Gal
	FN_ipsi	0.432	0.947	0.340	1.029	0.446	1.470	Gal
	CENT2_contra	0.865	0.947	1.154	0.530	0.475	0.925	Gal
	CENT3_contra	0.091	0.116	0.502	0.015	0.000	0.067	Gal
	CUL4-5_contra	0.091	0.316	0.290	0.015	0.144	0.015	Gal
	PYR_contra	0.046	0.100	0.011	0.000	0.000	0.005	Gal
	ANcr1_contra	0.023	0.116	0.028	0.061	0.058	0.200	Gal
	IP_contra	1.160	1.679	0.323	0.348	1.237	1.038	Gal

The abbreviation of nuclei refers to the annotation of the Allen Adult Mouse Atlases (http://atlas.brain-map.org/).

Table S4: Functional annotations of differentially labeled nuclei in the cortex, midbrain and hindbrain

	Nuclei	Type of network	Related function
CTX	MOp5_left	Gal	Motor related
	SSp-ll5_left	Gal	Sensory related
	SSp-tr5_right	Nts	Sensory related
	SSp-ll5_right	Common	Sensory related
MB	SCop_left	Gal	Sensory related
	VTA_left	Gal	Motor related
	SCdg_left	Gal	Motor related
	SCiw_left	Gal	Motor related
	SCig_left	Gal	Motor related
	APN_left	Gal	Motor related
	NPC_left	Gal	Motor related
	RN_left	Gal	Motor related
	DR_left	Gal	Behavioral state related
	ICc_right	Gal	Sensory related
	SNr_right	Gal	Motor related
	SCdg_right	Gal	Motor related
	SCig_right	Gal	Motor related
	PRC_right	Gal	Motor related
	APN_right	Gal	Motor related
	EW_right	Gal	Motor related
	IF_right	Gal	Behavioral state related
	DR_right	Gal	Behavioral state related
	MRN_right	Gal	Motor related
	PAG_right	Gal	Motor related
	PPN_right	Gal	Motor related
	MEV_left	Common	Sensory related
	CUN_left	Common	Motor related
	VTA_right	Common	Motor related
P	NLL_left	Gal	Sensory related
	CS_left	Gal	Behavioral state related
	V_right	Gal	Motor related
	RPO_right	Gal	Behavioral state related
	SOCm_left	Nts	Sensory related
	PB_left	Common	Sensory related
	KF_left	Common	Sensory related
	B_left	Common	Motor related
	PCG_left	Common	Motor related
	PRNc_left	Common	Motor related
	SLD_left	Common	Behavioral state related
	PB_right	Common	Sensory related
	SOCl_right	Common	Sensory related
	B_right	Common	Motor related
	PCG_right	Common	Motor related
	PRNc_right	Common	Motor related

	SUT_right	Common	Motor related
	LC_right	Common	Behavioral state related
	LDT_right	Common	Behavioral state related
	SLD_right	Common	Behavioral state related
MY	CU_left	Gal	Sensory related
	ECU_left	Gal	Sensory related
	SPVI_left	Gal	Sensory related
	SPIV_left	Gal	Motor related
	x_left	Gal	Motor related
	SPIV_right	Gal	Motor related
	SUV_right	Gal	Motor related
	IRN_right	Nts	Motor related
	AMBv_left	Nts	Motor related
	PGRNd_left	Nts	Motor related
	GRN_left	Common	Motor related
	IRN_left	Common	Motor related
	MARN_left	Common	Motor related
	MDRNd_left	Common	Motor related
	MDRNv_left	Common	Motor related
	PARN_left	Common	Motor related
	PGRNl_left	Common	Motor related
	PRP_left	Common	Motor related
	PPY_left	Common	Motor related
	MV_left	Common	Motor related
	XII_left	Common	Motor related
	RM_left	Common	Behavioral state related
	RPA_left	Common	Behavioral state related
	RO_left	Common	Behavioral state related
	GRN_right	Common	Motor related
	MARN_right	Common	Motor related
	MDRNd_right	Common	Motor related
	MDRNv_right	Common	Motor related
	PARN_right	Common	Motor related
	PGRNl_right	Common	Motor related
	MV_right	Common	Motor related
	XII_right	Common	Motor related
	RM_right	Common	Behavioral state related
	RPA_right	Common	Behavioral state related
	RO_right	Common	Behavioral state related

The abbreviation of nuclei refers to the annotation of the Allen Adult Mouse Atlases (http://atlas.brain-map.org/).

Abbreviation

Atf3	activating transcription factor 3
CB	cerebellum
CL	central lateral nucleus of the thalamus
CNU	cerebral nuclei
CTX	cerebral cortex
DMX	dorsal motor nucleus of the vagus nerve
DRG	dorsal root ganlion
DRL	dorsal raphe nucleus, lateral part
Gal	galanin
GFP	green fluorescent protein
GRN	gigantocellular reticular nucleus
HY	hypothalamus
ILM	intralaminar nuclei of the dorsal thalamus
int	internal capsule
MARN	magnocellular reticular nucleus
MB	midbrain
MD	mediodorsal nucleus of thalamus
MED	medial group of the dorsal thalamus
MEV	midbrain trigeminal nucleus
MOp	primary motor cortex
MTN	midline group of the dorsal thalamus
MY	medulla
Nts	neurotensin
NTS	nuclei of the solitary tract
P	pons
PAG	periaqueductal gray
DLPAG	dorsolateral PAG
DMPAG	dorsomedial PAG
LPAG	lateral PAG
VLPAG	ventrolateral PAG

PB		parabrachial nucleus
PDR		posterodorsal raphe nucleus
PF		parafascicular nucleus
PO		posterior complex of the thalamus
PPN		pedunculopontine nucleus
PRNc		pontine reticular nucleus, caudal part
py		pyramid
RM		nucleus raphe magnus
RN		red nucleus
RO		nucleus raphe obscurus
RPA		nucleus raphe pallidus
RT		reticular nucleus of the thalamus
RVM		rostral ventromedial medullar
scp		superior cerebellar peduncles
sctv		ventral spinocerebellar tract
SSp		primary somatosensory cortex
	SSp-ll	SSp, lower limb
	SSp-tr	SSp, trunk
TH		thalamus
VAL		ventral anterior-lateral complex of the thalamus
VNC		vestibular nuclei
VPL		ventral posterolateral nucleus of the thalamus
VPM		ventral posteromedial nucleus of the thalamus

Materials and Methods

Animals

Two transgenic mouse lines that expressing Cre recombinase under the *Gal* or *Nts* promoter were used. The *Gal*-Cre mice (STOCK Tg(*Gal*-cre)K187Gsat/Mmucd, 031060-UCD) were initially imported from the Mutant Mouse Regional Resource Center (1). The *Nts*-Cre mice (B6;129-*Nts*$^{tm1(cre)Mgmi}$/J mice; Jackson Laboratory, Stock No. 017525) were acquired from the Jackson laboratory (2). Only male transgenic mice were used. All mice were raised on a 12-hour light/dark cycle (lights on at 7:00 am) at 22 °C~26 °C with *ad libitum* food and water. All behavioral tests were carried out during the light phase. Experiments were performed according to the guidelines of the Committee for Research and Ethical Issues of the International Association for the Study of Pain, and were approved by the Committee of Use of Laboratory Animals and Common facility, the Center for Excellence in Brain Science and Intelligence Technology, CAS, and the Guangdong Institute of Intelligence Science and Technology.

Viral tracer preparation

The H129ΔTK-TT viral tracer was generously provided by Professor David J. Anderson (California Institute of Technology, Pasadena, CA). H129ΔTK-TT viruses were mass-produced by infecting Vero cells grown in T75 tissue culture flasks. After infected cells showed a prominent cytopathic effect (~2 days), medium containing the viruses was collected, centrifuged to remove cell debris (7,000 g for 10 min). The supernatant was passed through a 0.22 μm filter, and finally centrifuged at 50,000 g/3 hours using Beckman Avanti J-26SXP Ultracentrifuge. The virus pellet was resuspended overnight at 4 °C in a

small amount of cold phosphate buffer saline (PBS). Dissolved viruses were aliquoted into 3 µl and stored at -80 °C.

The titer of viral stocks was determined using standard plaque assay on Vero cells. Briefly, the assay was performed by serially diluting virus in Dulbecco's Modified Eagle Medium (DMEM) (Gibco) supplemented with 2% fetal bovine serum (Life Technologies) (2% DMEM) and overlaying infected cells with medium containing 2% fetal bovine serum, antibiotics (North China Pharmaceutical Co.), and 1% agarose (Biowest). Plaques were identified using neutral red staining and/or fluorescence microscopy. The titer of H129ΔTK-TT viral stocks was ~ 6×10^9 PFU/ml. A fresh aliquot of stock virus was thawed and used for each experiment.

Surgery for viral injection into the DRG

HSV infection was conducted in the laboratory at biosafety level 2. HSV was injected into the L5 DRG through a glass micropipette attached to a syringe driven by a Stoelting *kd* scientific pump. The syringe was mounted on an extended arm of a stereotaxic frame (RWD Life Science Co., Ltd) swung to the outside at a 30° angle. A volume of 850 nl of the viral vector solution was taken up into the micropipette. The micropipette was loaded separately with this volume for each injection.

Animals were anesthetized by isoflurane (RWD Life Science Co., Ltd) and mounted on a custom spine stabilizer (RWD Life Science Co., Ltd). Following an incision along the dorsal midline, the L5 DRG was exposed by removal of the lateral processes of the vertebrae. The glass micropipette was inserted into the exposed DRG. After a delay of 3 min to allow sealing of the tissue around the glass capillary tip, 800 nl virus solution was

injected at a rate of 80 nl/minute. After a further delay of 5 min, the micropipette was removed. The residual of viral vector solution in the micropipette was discarded. Then, 1 mg/kg bortezomib (EMD Millipore Corp.) at the concentration of 0.1 mg/ml was administrated by intradermal injection. Animals were allowed to survive for 7 days prior to further experiments.

AAV2/8-DIO-CAG-EYFP (titer: 1.00E+12 v.g./ml, Brain Case, Shenzhen, China) injection was conducted in the laboratory at biosafety level 1. The procedure was the same as injection of HSV except animals were allowed to survive for 3 weeks prior to further experiments.

Inducing and examination of c-Fos

Mice were handled and acclimated to the experimental environment for 4 days, then housed separately for 24 hours to reduce the background of c-Fos expression. To examine c-Fos expression induced by noxious heat stimuli, each mouse was put on the hot-plate with the temperature setting at 45 °C or room temperature for 5 min. To examine the c-Fos expression induced by histamine administrated at the hind paw, animals were anesthetized by isoflurane (RWD Life Science Co., Ltd) for a short time, then 10 μl of histamine (Sigma-Aldrich) at the concentration of 25 mg/ml or saline at the same volume was delivered into the left hind paw of each mouse. To examine the c-Fos expression induced by histamine administrated at the back neck, mice were briefly removed from the test chamber and given intradermal injection at the back neck with histamine (500 μg/50 μl) or saline at a volume of 50 μl. The perfusion was carried out 1.5-2 hours after stimuli.

Immunofluorescence staining

Mice were perfused with saline followed by 4% paraformaldehyde (PFA, Sigma-Aldrich). After the perfusion, the brain, spinal cord and/or DRG were dissected, and post-fixed in 4% PFA for overnight at 4 °C, followed by dehydration in 30% sucrose (Sinopharm Chemical Reagent Co., Ltd.). Free-floating sections of the brain (30 μm) were prepared for immunostaining. The cryostat sections of the DRG (10 μm) and spinal cord (20 μm) were mounted on slides immediately after sectioning. Tissue sections were blocked for 1 hour at room temperature in 0.5% Triton X-100 (Sigma-Aldrich) in PBS with 10% normal donkey serum (Jackson ImmunoResearch Inc.) and 0.1% gelatin (Sinopharm Chemical Reagent Co., Ltd.), followed by incubating with primary antibodies at 4 °C overnight and secondary antibodies at room temperature for 1 hour. The primary antibodies against RFP (1:1000, rabbit; MBL) and c-Fos (1:4000, Rb; CST) were used. The secondary antibodies were Cy3-conjugated donkey against rabbit antibodies (1:100; Jackson ImmunoResearch Inc.). Free-floating sections were counterstained with a fluorescent Nissl stain, Neuro Trace 435/455 (1:1000; Invitrogen) at room temperature for 1 hour.

Images were taken using an Olympus VS120 high-throughput microscope fitted with a 10× objective lens. Cell segmentation was carried out by particle analysis using Fiji (NIH). The results were manually corrected.

RNAscope ISH combined with immunofluorescence staining

The DRG slides were pretreated with hydrogen peroxide at room temperature for 10 min and washed with DEPC-ddH_2O twice. Then, slides were slowly immersed into boiling retrieval regent for 5 min and rinsed in the DEPC-ddH_2O. Then, slices were treated with

ethanol for 3 min and dry completely at room temperature. Protease digestion was performed in the 40 °C hybridization oven for 10-15 min and rinsed in the DEPC-ddH_2O twice. Then the slides were hybridized with the pre-warmed probe at 40 °C for 2 hours. TSA-based signal amplification (570, 690 or FITC) at 40 ℃ for 30 min was followed, and the slices next were incubated with primary antibodies at 4 ℃ for overnight and secondary antibodies at room temperature for 1 hour. Finally, slides were mounted and image.

3D reconstruction and registration of brain slices

Fluorescent images at the interval of 120 μm were captured tile by tile so as to be assembled together as whole-brain images. TIFF files with signals of Nissl bodies were used for registration of assembled brains into 3D Allen CCFv3. The brain slices were registered to the Allen CCFv3 to depict the boundaries of brain regions and nuclei in slices. A reconstruction method of brain slices, which took brain atlas as the reference, was used to solve the problem of axial migration, which was also called z-shift problem. The reconstructed volume of brain slices could be well matched to the reference atlas in shape, size and position (3).

The OTSU algorithm was applied for image segmentation of labeled neurons in the brain. The binarized images were submitted for particle analysis using the Fiji (ImageJ, NIH). Thus, the coordinate of labeled neurons was determined. The results were checked manually using the LabelMe (http://labelme.csail.mit.edu/Release3.0/). Cell number in each nucleus was determined based on the registered coordinate of labeled neurons using a Python script written by ourselves. The Amira-Avizo Software (Thermoscientific) was used for data visualization.

Nuclei silencing and behavior tests

For inhibiting the neuronal activity of RN or NST, AAV2/9-Ef1α-DIO-hM4Di-mCherry (titer: 1.20E+13 v.g./ml, BrainVTA, Wuhan, China) mixed with AAV2/1-hSyn-Cre (titer: 1.05E+13 v.g./ml, BrainVTA, Wuhan, China) at the ratio of 10:1 was injected into left RN or NST. AAV2/9-Ef1α-DIO-mCherry (titer: 5.02E+12 v.g./ml, BrainVTA, Wuhan, China) mixed with AAV2/1-hSyn-Cre (titer: 1.05E+13 v.g./ml, BrainVTA, Wuhan, China) at the ratio of 10:1 was injected as a control. Injection sites for RN and NST were bregma: -3.39 mm, lateral: -0.75 mm, depth: -3.74 mm and bregma: -7.30, lateral: -0.51, depth: -4.36, respectively. All viruses were injected with a volume of 30 nl/site. Behavioral tests were performed at least 2 weeks after viral injection. Mice received intraperitoneal injection of 1 mg/kg Clozapine-n-oxide (CNO) (Sigma-Aldrich) 30 min before behavioral tests.

Hot plate test

Mice were handled and acclimated to the experimental environment for 3-4 days. On the test day, mice were put on the hot-plate with the temperature setting at 52 °C. The latency to jump, shake or lick the hind paw was measured. The cutoff time was set at 30 seconds.

Hargreaves test

Mice were habituated in plastic chambers, the radiant light was applied to the right hind paw of mice when they were resting quietly, and the latency to paw withdraw was measured. The cutoff time was set at 20 seconds.

Itch behavioral test

Before experiments, mice were given 30 min to acclimate to the test chamber before treatment. Mice were briefly removed from the test chamber and given intradermal

injection at the back neck with histamine (500 μg/50 μl), 5-HT (10 μg/50 μl) or saline at a volume of 50 μl. Hindlimb scratching behavior directed toward the injection site was observed for 30 min. A bout of scratching was defined as a lifting of the hindlimb and a fall back of the limb back to the floor. Scratching behavior was qualified by counting the number of scratching bouts over the 30 min recording period. All videos were analyzed by trained investigators blinded to the experimental treatment of the animals.

Measurement of heart rate and blood pressure

Mice were handled and acclimated to the experimental environment for 2 days. Then, mice were restrained and warmed in a soft tube. Indirect blood pressure and heart rate measurements were performed in conscious, restrained mice by tail-cuff plethysorgraphy (BP-2010A, Softron Biotechnology, Beijing, China). The machine monitored the state of an animal automatically and started measurements once the animal was calm down. We used systolic blood pressure for analysis since it was more precise than diastolic blood pressure when using the tail-cuff method. Heart rate was quantified by beats per min (bpm).

Open field test

Mice were acclimated to the experimental environment for 1 hour. Then mice were put into an open field (45 × 45 cm) for measurement of exploratory locomotor activity in a 15 min period by a Digiscan apparatus (Accuscan Electronics). The total distance of moving during the whole procedure was recorded. Mean velocity was determined by the distance of moving in a period of time.

Rotarod

Mice from each group were pretrained for adaptation. On the test day, mice were acclimated to the experimental environment for 1 hour. Then locomotor coordination and

balance were measured by placing mice on an accelerating, 3 cm diameter and rotating drum for three trials. The minimum interval between trials was 30 min. The rotarod started at 4 rpm and increased to 30 rpm over a 5 min period. The latency to fall was recorded.

Statistical analysis

Statistical analysis was performed using Prism 8 and RStudio v1.2.5019. Pearson correlation was used to determine the similarity of labeling pattern among neural networks. The data were compared using unpaired t-test. The cutoff for significance was held at $P = 0.05$.

SI Reference

1. Z. Wu, A. E. Autry, J. F. Bergan, M. Watabe-Uchida, C. G. Dulac, Galanin neurons in the medial preoptic area govern parental behavior. *Nature* **509**, 30 (2014).
2. G. M. Leinninger *et al.*, Leptin action via neurotensin neurons controls orexin, the mesolimbic dopamine system and energy balance. *Cell Metab.* **14** (2011).
3. H. Ni *et al.*, A robust image registration interface for large volume brain atlas. *Scientific reports* **10**, 17 (2020).